

Comparative Study of Bulk and Supported V–Mo–Te–Nb–O Mixed Metal Oxide Catalysts for Oxidative Dehydrogenation of Propane to Propylene

Zhen Zhao, Xingtao Gao, and Israel E. Wachs*

In Situ Molecular Characterization and Catalysis Laboratory, Department of Chemical Engineering, Lehigh University, Bethlehem, Pennsylvania 18015.

Received: July 17, 2002; In Final Form: February 24, 2003

Bulk V–Nb–O, Mo–Nb–O, Te–Nb–O, and V–Mo–Te–Nb–O mixed metal oxides were synthesized and characterized with Raman spectroscopy, XRD, and BET methods. The interaction of the V and Mo cations with the Nb₂O₅ lattice followed three stages: (1) cations were initially incorporated into the Nb₂O₅ lattice forming a solid solution or compound as well as on the Nb₂O₅ surface, (2) a two-dimensional surface cation overlayer was formed after saturation of the solid solution, and (3) microcrystalline metal oxide phases (e.g., V₂O₅ and MoO₃) were formed after completion of the two-dimensional surface cation monolayer. The catalytic properties of these bulk mixed metal oxides were investigated for the oxidative dehydrogenation (ODH) of propane to propylene, and their activity follows the trend: V–Nb–O > Mo–Nb–O ≫ Nb₂O₅ > Te–Nb–O. The highest propane conversions and propylene yields were found when the two-dimensional surface metal oxide monolayers were formed, which suggests that the surface metal oxide species are the surface active sites in these bulk mixed metal oxide catalysts for propane ODH. Furthermore, the number of surface active sites present in the bulk mixed metal oxides was determined by comparative studies between the bulk mixed metal oxides and the corresponding model Nb₂O₅-supported metal oxides. These numbers can be used further for the calculation of the TOF (turn-over-frequency) values and quantitative comparison of the catalytic behavior of the different bulk mixed metal oxide catalysts for propane ODH. The catalytic results over the model Nb₂O₅-supported metal oxides demonstrate that the propane ODH reaction is structure insensitive because the TOF is independent of the number and the structure of surface active sites. The composition and calcination temperature of the bulk mixed metal oxide catalysts affects the surface density of the active sites, which controls their catalytic behavior for propane ODH.

1. Introduction

Mixed metal oxide catalysts consisting of bulk and/or supported metal oxides are an important class of catalytic materials employed in numerous fundamental studies and industrial applications.^{1–8} Supported metal oxides consist of a two-dimensional metal oxide overlayer on the surface of an oxide substrate (support). The supported metal oxide binds to the oxide support via bridging M–O–S bonds (M = metal and S = support), which are primarily formed by reaction of the MO_x with surface hydroxyl groups of the oxide support. For supported metal oxides, it is reasonable to normalize the reactivity per MO_x because all the MO_x sites are exposed to the reactant molecules when the MO_x loading is below monolayer surface coverage (100% dispersion). Thus, calculation of the turnover frequency (TOF) under the assumption that all the surface MO_x sites are active sites is an appropriate approach.^{4–6} However, bulk mixed metal oxides are significantly more complicated and consist of both bulk three-dimensional structures and the surface active sites, with the surface density and nature of the latter generally unknown. Furthermore, the catalytic contributions from the bulk metal oxide sites, which are not directly exposed to the reactant molecules, are not fully understood and have not been quantified. Thus, it is very difficult to quantify the number of active sites present in bulk

mixed metal oxide catalysts and to calculate their TOF values. Only one previous investigation of alkane oxidation focused on quantifying the TOF values of bulk V–Nb–O mixed metal oxide catalysts.⁹

Oxidative dehydrogenation (ODH) of propane to propylene is energetically favorable and has attracted much attention in recent years. Vanadium^{9–15} and molybdenum^{16–18} oxides have been widely used as active components both in bulk and in supported mixed metal oxides for propane ODH. Many recent supported metal oxide studies^{9–22} have investigated the effects of metal oxide loading, structure of the surface metal oxide species, oxide supports, and promoters. It was found that the oxide supports and promoters largely affect the activity and selectivity of the supported vanadia or molybdena species for propane ODH via modification of the redox and acid–base properties of the catalysts.^{23–26} For propane ODH over vanadia supported on different oxide supports, the specific catalytic activity was found to qualitatively follow the reducibility patterns obtained by H₂-TPR, whereas their selectivity follows a different order.^{23,24} These results indicate that the nature of the oxide support strongly affects the selectivity/activity of the supported vanadia catalysts. Contradictory results have also been reported by other authors,¹⁹ who concluded that the turnover frequency rates do not depend on the specific identity of the support, but on the domain size of the surface VO_x species and that intermediate surface VO_x domain sizes result in maximum activity.

* Corresponding author. Prof. Israel E. Wachs, Sinclair Lab. # 7, 7 Asa Drive, Lehigh University, Bethlehem, PA 18015. Telephone: (610)-758-4274. Fax: (610)-758-6555. E-mail: iew0@lehigh.edu.

The catalytic behavior of isolated and polymeric surface species on supports for alkane oxidation is still under discussion.^{9–27} Watling et al.⁹ investigated niobia-supported vanadium oxide and bulk V–Nb–O mixed metal oxide catalysts for propane ODH and found that all the samples possessed similar TOF values when the reaction rates were normalized to the concentration of surface vanadia. The results suggest that variations in the chemical environment of the surface vanadium cation do not cause significant changes in catalytic activity per surface active site (TOF). The propane ODH over V₂O₅/Al₂O₃ catalysts was reported by Eon et al.,²⁸ and the same selectivity versus conversion was obtained. The activity, if converted to TOF values from their results, is only slightly higher at high surface vanadia loadings (less than a factor of 2). Very recently, Gao et al.²⁷ studied propane ODH over ZrO₂-supported vanadium oxide catalysts. The results revealed that both polymerized and isolated surface vanadia species are active sites for propane oxidation and the specific catalytic reactivity (TOF) is independent of the surface density of the two-dimensional vanadia overlayer on the ZrO₂ support. Similarly, for ethane ODH, the TOF value for ethane oxidation remains essentially constant for V₂O₅/Al₂O₃ catalysts at different vanadia loadings.^{29–31} On the basis of the study of TOF and product distribution, Oyama and Somorjai^{32,33} concluded that for ethane oxidation over silica-supported vanadia catalysts, the selective oxidation for ethylene and acetaldehyde formation is structure insensitive whereas the reaction for CO_x formation is structure sensitive. In contrast, some other studies concluded that the polymerized surface MO_x species on the oxide support are more active than isolated MO_x species for propane ODH (18–22).

In the present study, bulk V–Nb–O, Mo–Nb–O, Te–Nb–O, and V–Mo–Te–Nb–O mixed metal oxides were synthesized by using Nb₂O₅, the major component, as a host matrix for the bulk mixed metal oxide catalysts because niobia is very inactive for propane activation.⁹ These bulk mixed metal oxide catalysts were characterized with ambient and in situ Raman, XRD, and BET. Furthermore, comparative studies between these bulk mixed metal oxides and their corresponding model Nb₂O₅-supported metal oxides were undertaken to obtain additional insight into the molecular structure–reactivity/selectivity relationships of these bulk mixed metal oxide catalysts.

2. Experimental Section

2.1. Catalyst Preparation. 2.1.1. Bulk Mixed Metal Oxides.

Ammonium vanadate (NH₄VO₃) (Alfa-AESAR, 99.93% purity), ammonium heptamolybdate ((NH₄)₆Mo₇O₂₄·4H₂O) (Matheson Coleman & Bell, 99.9%), telluric acid (H₂TeO₄·2H₂O) (Alfa Aesar), and niobium oxalate (Nb(HC₂O₄)₅) (CBMM, 99.5% purity) were used as starting materials for introducing the V, Mo, Te, and Nb oxide precursors, respectively. The bulk V–Nb–O, Mo–Nb–O, Te–Nb–O, and V–Mo–Te–Nb–O mixed metal oxides were prepared by similar methods previously described.³⁴ For example, for preparing the V–Nb–O mixed metal oxides an aqueous mixture containing V and Nb metal ions in the appropriate ratio was prepared by mixing corresponding aqueous solutions of the starting materials. The aqueous mixture was subsequently evaporated to dryness by stirring and heating at 150 °C. Finally, the dry precursor was calcined in air for 2 h at 600 °C to form bulk mixed metal oxide catalysts. Each catalyst is denoted as *x*% M–Nb–O (M = V, Mo, or Te; *x* = 1, 5, 10, 20), where *x*% represents the weight percentage of the metal oxide in the Nb₂O₅ matrix. As comparison to the mixed oxides, pure V₂O₅, MoO₃, and TeO₂ were obtained by calcination of ammonium vanadate, am-

monium heptamolybdate, and telluric acid at 600 °C for 2 h, whereas the pure Nb₂O₅ was prepared by drying an aqueous solution of niobium oxalate with subsequent calcination at 600 °C for 2 h.

2.1.2. Nb₂O₅-Supported Metal Oxide Catalysts. The Nb₂O₅ support (*S*_{BET} = 57 m²/g) was obtained by calcination of niobium oxide hydrate (Nb₂O₅·*n*H₂O) (CBMM, 99.9% purity) at 500 °C in air for 10 h.

The supported V₂O₅/Nb₂O₅ catalysts were prepared by incipient-wetness impregnation of the Nb₂O₅ support with 2-propanol solutions of vanadium isopropoxide (VO(O–*i*Pr)₃, Alfa-Aesar 97% purity). The preparation was performed inside a glovebox with continuously flowing N₂. After impregnation, the samples were kept inside the glovebox with flowing N₂ for overnight. The samples were further dried in flowing N₂ at 120 °C for 1 h and calcined in flowing air at 450 °C for 2 h.³⁵

The supported MoO₃/Nb₂O₅ and TeO₂/Nb₂O₅ samples were prepared by incipient-wetness impregnation of the Nb₂O₅ support with aqueous solutions of ammonium heptamolybdate (Matheson Coleman & Bell, 99.9%) and telluric acid (H₂TeO₄·2H₂O, Alfa Aesar), respectively. After impregnation, the samples were dried under ambient conditions for 48 h and calcined in air at 450 °C for 2 h.

2.2. BET Surface Area. The BET surface area of each sample was measured by nitrogen adsorption/desorption isotherms with a Micromeritics ASAP 2000.

2.3. X-ray Diffraction. Powder X-ray diffraction (XRD) data were recorded on a Siemens D-5000 diffractometer operated at 40 kV and 40 mA using nickel-filtered Cu K α radiation.

2.4. Raman Spectroscopy. Raman spectra of the hydrated and dehydrated samples were obtained in the 100–1200 cm^{–1} region with the 514.5 nm excitation of an Ar⁺ ion laser (Spectra Physics, model 164). The scattered radiation from the sample was directed into an OMA III (Princeton Applied Research, model 1463) optical multichannel analyzer with a photodiode array detector cooled thermoelectrically to –35 °C. The samples were pressed into self-supporting wafers. The Raman spectra of the hydrated samples were collected by rotating the sample at ~2000 rpm under ambient conditions. The Raman spectra of the dehydrated samples were recorded at room temperature after heating the sample in flowing O₂ at 450–500 °C for 1 h in a stationary quartz cell.^{35,36}

2.5. Propane Oxidation. Propane oxidation was carried out in an isothermal fixed-bed differential reactor (Pyrex tubing, 1/4 in. o.d. and 1 ft long) using 30–100 mg of catalyst at atmospheric pressure with reaction temperatures varying from 250 to 550 °C. The reactant gas mixture of C₃H₈/O₂/He has a molar ratio of 2.5/20/27.5 with a flow rate of 50 mL/min, unless otherwise stated. The reactor effluent was analyzed by an on-line Hewlett-Packard Gas Chromatograph 6890 Series equipped with both TCD and FID detectors. A Carboxene-1000 packed column and a Supelco capillary column (PQ1334-04) were employed in parallel for the TCD and FID, respectively.²⁷ The samples were pretreated in a flowing O₂/He gas mixture at 450 °C for 0.5 h before each run. The specific catalytic activity values, turnover frequency (TOF, the number of propane molecules converted per M atom per second), were obtained at reaction temperatures of 400 and 450 °C for vanadia- and molybdena-containing samples, respectively. The number of active surface V, Mo, and Nb atoms per nm² for the pure V₂O₅, Nb₂O₅, and MoO₃ crystalline phases was determined by quantitative chemisorption of 2-propanol and methanol.^{37,38}

TABLE 1: BET Surface Areas of Bulk and Supported Metal Oxide Samples

bulk mixed metal oxides		supported metal oxides	
sample	surface area (m ² /g)	sample	surface area (m ² /g)
Nb ₂ O ₅	18.2	Nb ₂ O ₅	57
1% V–Nb–O	25.0	1% V ₂ O ₅ /Nb ₂ O ₅	42.6
5% V–Nb–O	15.2	2% V ₂ O ₅ /Nb ₂ O ₅	41.9
10% V–Nb–O	15.2	3% V ₂ O ₅ /Nb ₂ O ₅	40.7
20% V–Nb–O	6.7	4% V ₂ O ₅ /Nb ₂ O ₅	39.8
V ₂ O ₅	1.9	5% V ₂ O ₅ /Nb ₂ O ₅	34.7
		6% V ₂ O ₅ /Nb ₂ O ₅	33.6
1% Mo–Nb–O	16.0	8% V ₂ O ₅ /Nb ₂ O ₅	30.2
5% Mo–Nb–O	18.6	V ₂ O ₅	1.9
10% Mo–Nb–O	19.2		
20% Mo–Nb–O	22.3	1% MoO ₃ /Nb ₂ O ₅	54.0
MoO ₃	0.8	2% MoO ₃ /Nb ₂ O ₅	53.1
		3% MoO ₃ /Nb ₂ O ₅	51.2
1% Te–Nb–O	22.4	4% MoO ₃ /Nb ₂ O ₅	50.2
5% Te–Nb–O	18.5	5% MoO ₃ /Nb ₂ O ₅	49.1
10% Te–Nb–O	15.4	6% MoO ₃ /Nb ₂ O ₅	47.0
20% Te–Nb–O	0.9	8% MoO ₃ /Nb ₂ O ₅	43.0
TeO ₂	1.7	10% MoO ₃ /Nb ₂ O ₅	40.4
		20% MoO ₃ /Nb ₂ O ₅	30.2
		MoO ₃	0.8

3. Results

3.1. BET Surface Areas. The BET surface areas of the three bulk mixed metal oxides systems (V–Nb–O, Mo–Nb–O, and Te–Nb–O) and the two corresponding Nb₂O₅-supported vanadia and molybdena systems are presented in Table 1. For the Nb₂O₅-supported metal oxide systems, their surface areas slightly decrease with increasing surface vanadia and molybdena coverage. The surface areas of the pure Nb₂O₅ and the Nb₂O₅ support are different due to the different precursors and calcination treatments of these samples (see catalyst preparation-section 2.1). The pure V₂O₅, MoO₃, and TeO₂ possess very low surface areas (<2 m²/g) and the surface area of pure Nb₂O₅, obtained by calcination of niobium oxalate, is much higher (18.2 m²/g). For the bulk V–Nb–O and Te–Nb–O mixed oxide systems, the surface area initially increased with the addition of vanadia or telluria, but it subsequently decreased at high metal oxide loading. For the bulk Mo–Nb–O mixed oxide system, the surface area initially slightly decreased at low molybdena content and then it increased with increasing molybdena content.

3.2. XRD of Bulk Mixed Metal Oxides. The XRD analyses of the bulk V–Nb–O and Mo–Nb–O mixed metal oxides are presented in Table 2. The XRD pattern of pure Nb₂O₅ is the TT phase with a hexagonal crystal structure.³⁹ When low amounts of vanadia or molybdena (≤5 wt %) were doped into the Nb₂O₅ matrix, the XRD patterns obtained were very similar to that of pure Nb₂O₅ (TT) and the *d* values only changed slightly. These results indicate that the solid solutions of the bulk V_xNb_{2-x}O₅ and Mo_xNb_{2-x}O₅ mixed metal oxide phases are isostructural with Nb₂O₅ (TT). In the V–Nb–O system, a very different XRD pattern was observed when the V₂O₅ content reaches 10 wt % or higher. This phase was previously reported as an unknown new phase¹² but has been recently assigned to V₄Nb₁₈O₅₅.⁴⁰ For the Mo–Nb–O system with MoO₃ contents of 10% or greater, the XRD patterns are consistent with the Nb₂O₅ (TT) solid solution. In addition, very weak diffraction peaks due to crystalline MoO₃ were also observed, indicating the formation of a small amount of MoO₃ crystallites. Nevertheless, the intensities of the XRD diffraction peaks are very weak for both the bulk V–Nb–O and Mo–Nb–O mixed metal oxides with V₂O₅ or MoO₃ contents of 10% and greater, suggesting that poorly crystalline or amorphous phases are present in these catalytic materials.

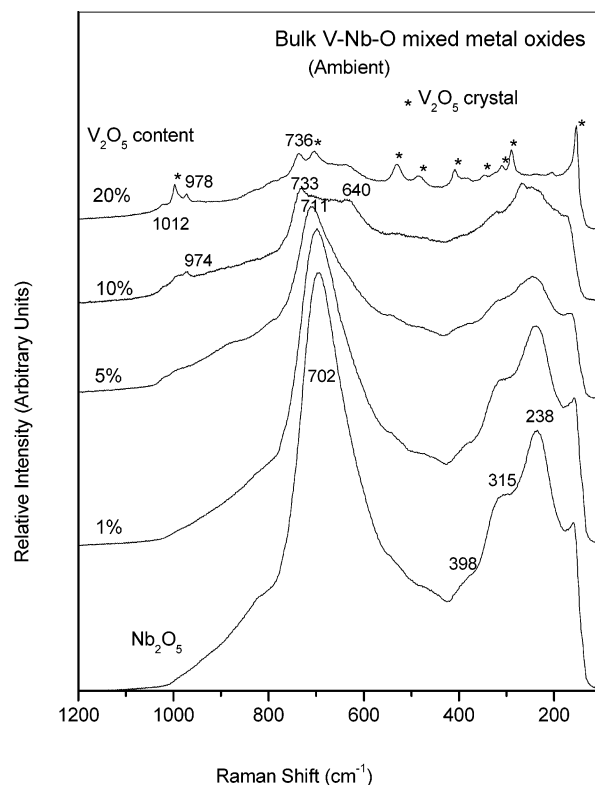


Figure 1. Raman spectra of bulk V–Nb–O mixed metal oxides under ambient conditions.

No XRD analysis was performed on the Nb₂O₅-supported metal oxides because the metal oxides were primarily present as amorphous two-dimensional metal oxide overlayers or very small crystallites (<4 nm) that are readily detectable by Raman spectroscopy (see below).

3.3. Raman Spectroscopy. **3.3.1. Raman Spectra of Nb₂O₅-Supported Metal Oxides.** The Raman spectra of Nb₂O₅-supported vanadia catalysts (not shown here for brevity), under ambient conditions, revealed that no crystalline V₂O₅ was detected for vanadia loadings below 5% V₂O₅/Nb₂O₅. A very weak Raman band at ~155 cm⁻¹, which is extremely strong for pure V₂O₅, was observed for 5% V₂O₅/Nb₂O₅, indicating the presence of a trace amount of microcrystalline V₂O₅. The intensity of the Raman band at 155 cm⁻¹ rapidly increased with increasing vanadia loading above 5% V₂O₅/Nb₂O₅. The results suggest that 5% V₂O₅/Nb₂O₅ corresponds to monolayer surface coverage.⁹ Under dehydrated conditions, pronounced Raman bands for the surface vanadia species were also observed: ~1035 and 1000 cm⁻¹ bands due to the terminal V=O vibrations of isolated and polymeric surface vanadia species, respectively.^{4-6,27}

The Raman spectra of Nb₂O₅-supported molybdena catalysts, under ambient conditions, were also measured (not shown here for brevity). A small Raman band appeared at around 815 cm⁻¹ for 8% MoO₃/Nb₂O₅, due to the presence of microcrystalline MoO₃, which suggests that the monolayer coverage of surface molybdena species has been slightly exceeded.³⁶ In addition, weak Raman bands were observed at ~960 and ~1000 cm⁻¹, which are due to hydrated and dehydrated surface MoO_x species, respectively.³⁶

3.3.2. Raman Spectra of Bulk Mixed Metal Oxides. The Raman spectra of the bulk V–Nb–O mixed metal oxides under ambient conditions are presented in Figure 1. Pure Nb₂O₅ (TT) possesses Raman bands at ~238, 315, and 702 cm⁻¹ and rather weak and broad bands from 800 to 1000 cm⁻¹. The Raman

TABLE 2: XRD of Bulk V–Nb–O and Mo–Nb–O Mixed Metal Oxides

samples	phase by XRD	cryst struct ^a	d_{001}	d_{200}	d_{100}	d_{035}
Nb ₂ O ₅	TT	H	3.8971		3.1180	
1% V–Nb–O	TT	H	3.8972		3.1078	
5% V–Nb–O	TT	H	3.9311		3.0974	
10% V–Nb–O	V ₄ Nb ₁₈ O ₅₅	O		3.9657		2.9959
20% V–Nb–O	V ₄ Nb ₁₈ O ₅₅	O		3.9833		2.9957
V ₂ O ₅		O	4.368	5.765	3.405 ₁₁₀ ^c	
1% Mo–Nb–O	TT	H				
5% Mo–Nb–O	TT	H	3.8803		3.0974	
10% Mo–Nb–O	TT + MoO ₃ ^b	H	3.9483		3.1293	
20% Mo–Nb–O	TT + MoO ₃	H	3.9483		3.1293	
MoO ₃		O	3.7736 ₁₁₀ ^d	3.2407 ₀₂₁ ^e		

^aNote: H: hexagonal; O: orthorhombic. ^bTrace amount. ^c3.405₁₁₀: 3.405 is the d value for the 110 plane. ^d3.7736₁₁₀: 3.7736 is the d value for the 110 plane. ^e3.2407₀₂₁: 3.240 is the d value for the 021 plane.

band at 702 cm⁻¹ was previously assigned to a slightly distorted NbO₆ structure (Nb–O vibration in Nb–O–Nb bridging bond).⁴¹ The Raman bands at ca. 315 and 238 cm⁻¹ are due to the angle deformation modes of O–Nb–O and bridging Nb–O–Nb bonds, respectively.^{41–44} The Raman bands at 702, 315, and 238 cm⁻¹ all shift upward with increasing vanadia content. The intensity of the Raman bands also decreases with increasing vanadia content because of the greater absorption of the incident laser light by the colored vanadia component. The oxidation states of V and Nb are the same, +5, but the radius of V⁵⁺ is much smaller than Nb⁵⁺.⁴⁵ When a small amount of vanadia is introduced into the Nb₂O₅ matrix (1% V–Nb–O and 5% V–Nb–O), the Raman spectra are very similar to that of pure Nb₂O₅ (TT), which further confirms the formation of a V_xNb_{2-x}O₅ solid solution. However, the Raman spectra under ambient conditions significantly changed when a medium amount of vanadia (10% V–Nb–O) was added to the Nb₂O₅ matrix. New Raman bands were observed at ~970 and ~1000 cm⁻¹ due to terminal V=O vibrations. The Raman bands at ca. 700 and 280 cm⁻¹ are (1) very broad, suggesting the presence of several types of bridging V–O–Nb and Nb–O–Nb bonds in this sample, and (2) significantly shifted to higher wavenumber due to structural distortions of the V_xNb_{2-x}O₅ solid lattice. From XRD (see above and Table 2) the crystalline V₄Nb₁₈O₅₅ compound was also shown to be present in this sample and, consequently, there are several types of bonds connecting V, Nb, and O. Microcrystalline V₂O₅ was detected by Raman in the 20% V–Nb–O sample, but not by XRD, which indicates that the V₂O₅ microcrystals are smaller than 4 nm, the lower detection limit of XRD.

The Raman spectra of the bulk V–Nb–O mixed metal oxides under dehydrated conditions are shown in Figure 2. Comparison of Figures 1 and 2 reveals that there is a significant shift in the band positions around 1000 cm⁻¹, indicating that these bands originate from surface metal oxide species.^{4–6} There are no detectable Raman bands in the 970–1000 cm⁻¹ region for pure Nb₂O₅ and 1% V–Nb–O, although the concentration of surface NbO_x species is relatively high in these two samples. For the 5% V–Nb–O sample, no clear peak was observed above 900 cm⁻¹ under ambient conditions whereas a new Raman band around 980 cm⁻¹ appeared under dehydrated conditions, which indicates that it originated from terminal surface V=O functionalities of the V_{2-x}Nb_{2-x}O₅ solid solution. At higher vanadia contents of 10% and 20% V–Nb–O, a new band at 1020 cm⁻¹ was observed after dehydration, which may be assigned to terminal surface V=O functionalities on the surface of the mixture of crystalline V₄Nb₁₈O₅₅ and possible amorphous V–Nb–O phases. Moreover, the Raman band at ~976 cm⁻¹ may be assigned to a bulk V=O functionality of crystalline

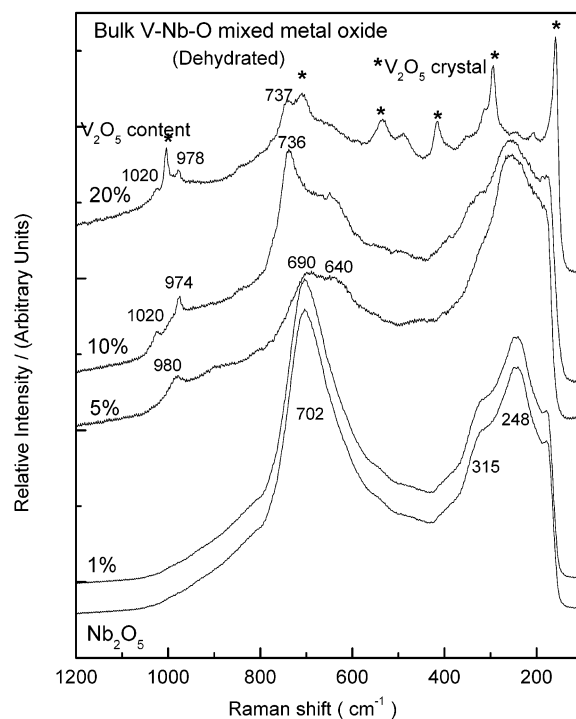


Figure 2. Raman spectra of bulk V–Nb–O mixed metal oxides under dehydrated conditions.

V₄Nb₁₈O₅₅ because it did not change position upon dehydration and its appearance coincided with appearance of V₄Nb₁₈O₅₅.

The Raman spectra of the bulk Mo–Nb–O mixed metal oxides under ambient conditions are presented in Figure 3. For the 1% and 5% Mo–Nb–O samples, the Raman features are very similar to Nb₂O₅ (TT), indicating the formation of Mo_xNb_{2-x}O₅ solid solution. The Raman band at ~700 cm⁻¹ shifts upward with increasing molybdena content, due to the distortion created by the incorporation of the Mo⁶⁺ cations into the Nb₂O₅ (TT) matrix. The Raman bands for the Nb₂O₅ (TT) solid solution are still observable for the 20% Mo–Nb–O sample. In addition, weak Raman bands are also present at ~980 and 815 cm⁻¹, due to hydrated surface Mo=O species and microcrystalline MoO₃ particles (<4 nm), respectively.³⁶ Upon a further increase of the content of molybdena to 40% Mo–Nb–O, multiple Raman bands of crystalline MoO₃ were observed and the band at ~980 cm⁻¹, due to surface MoO_x species, is still present.

The Raman spectra of the bulk Mo–Nb–O mixed metal oxides under dehydrated conditions are presented in Figure 4. Comparison of Figures 3 and 4 reveals the differences in the

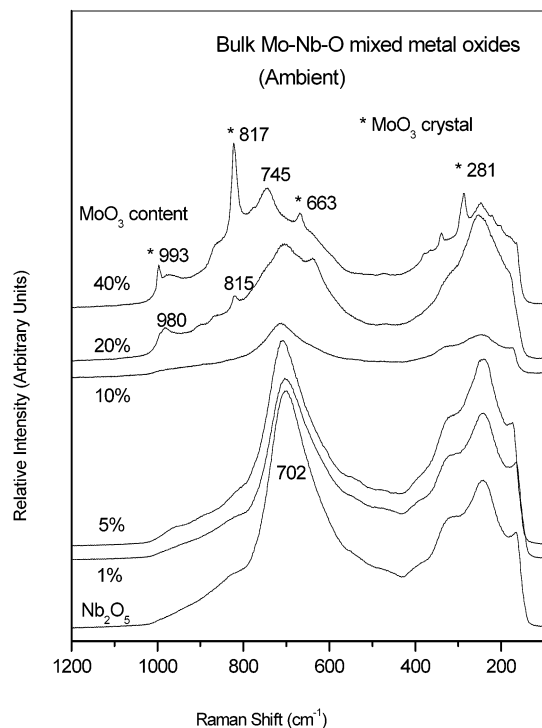


Figure 3. Raman spectra of bulk Mo–Nb–O mixed metal oxides under ambient conditions.

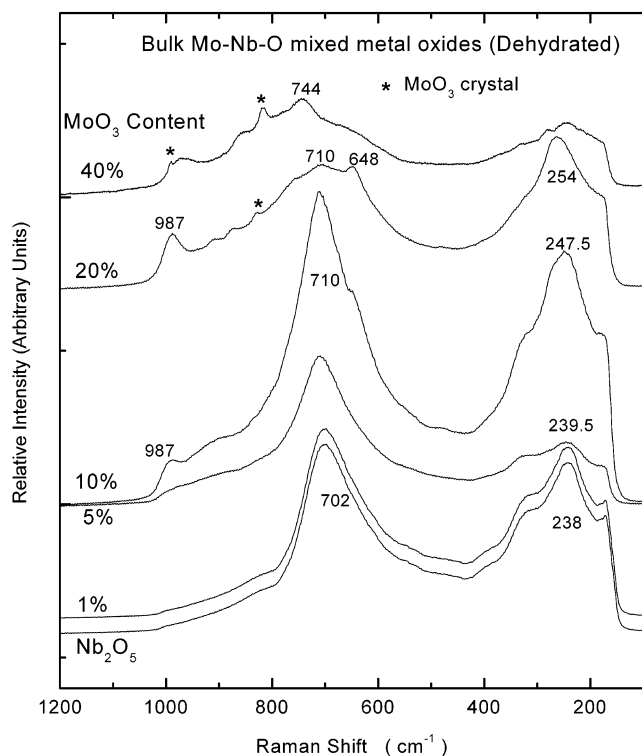


Figure 4. Raman spectra of bulk Mo–Nb–O mixed metal oxides under dehydrated conditions.

Raman features of the bulk Mo–Nb–O mixed oxides due to the presence of surface MoO_x species. For the 10% Mo–Nb–O sample, no Raman band around 980 cm⁻¹ was detected under ambient conditions whereas a Raman band at ~987 cm⁻¹ appeared under dehydrated conditions, indicating the presence of a surface Mo=O functionality. This Raman band cannot be due to terminal surface Nb=O vibrations because it is not present in the pure Nb₂O₅ and 1% and 5% Mo–Nb–O samples.

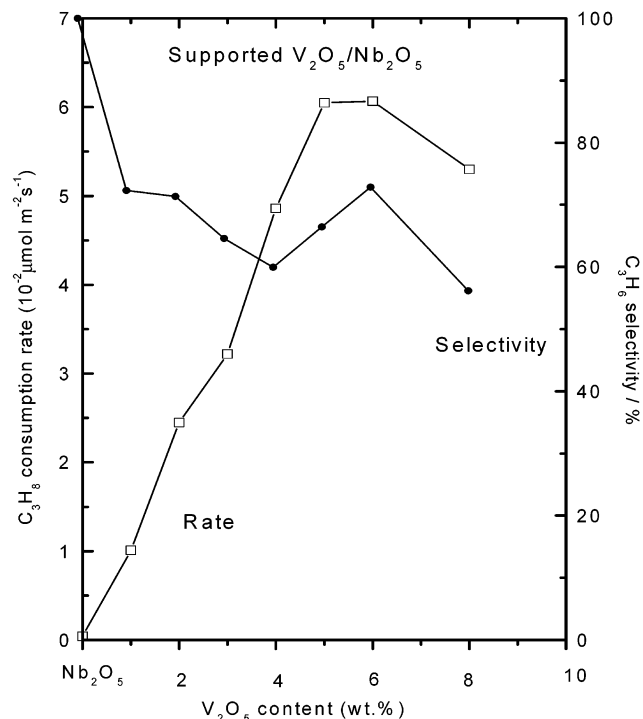


Figure 5. Oxidative dehydrogenation of propane over Nb₂O₅-supported vanadia metal oxides. Reaction at 400 °C; SF = 50 mL/min.

The relative intensity of the Raman signal for crystalline MoO₃ significantly decreased after the dehydration pretreatment at 500 °C due to the thermal broadening caused by local heating of the stationary sample spot by the laser beam.^{46,47}

The Raman spectra of the bulk Te–Nb–O mixed metal oxides under ambient and dehydrated conditions were recorded (not shown here for brevity). Similar to the Mo–Nb–O system, the Nb–O vibrations shift from ~700 to 735 cm⁻¹ with increasing Te oxide loading. For 20% Te–Nb–O, a broad shoulder at ~692 cm⁻¹ due to TeO₂ crystallites was observed, indicating the saturation of Te_xNb_{2-x}O₅ solid solution and the formation of the TeO₂ phase. Unfortunately, the surface telluria species is not observable by Raman spectroscopy.

3.4. Catalytic Activity for Propane ODH. **3.4.1. Catalytic Activity of Supported Metal Oxides.** The catalytic properties of the model Nb₂O₅-supported vanadia and molybdena catalysts were initially investigated to obtain additional insights into the catalytic nature of the bulk mixed metal oxides during propane ODH.

The catalytic properties of Nb₂O₅-supported vanadia for propane oxidative dehydrogenation at 400 °C are shown in Figure 5. The propylene selectivity for pure Nb₂O₅ is very high (almost 100%) at these reaction conditions, but the propane conversion is very low. For the Nb₂O₅-supported vanadia catalysts, the selectivity to propylene is rather similar (60–70%) over a wide range of propane conversions and vanadia content. The reaction rate for propane consumption linearly increases with increasing surface vanadia loading, reaches a maximum at 5% V₂O₅/Nb₂O₅, remains constant at 6% V₂O₅/Nb₂O₅ and markedly decreases with increasing vanadia content. The catalytic results reveal that ~5% V₂O₅/Nb₂O₅ corresponds to monolayer surface coverage and a small amount of V₂O₅ crystallites has no catalytic effect. However, significant amounts of crystalline V₂O₅ particles have a negative effect on propane ODH due to their intrinsic low surface area and covering of the surface vanadia sites. The catalytic properties of supported V₂O₅/Nb₂O₅ for propane ODH are summarized in Table 3. The

TABLE 3: Catalytic Properties of Supported V₂O₅/Nb₂O₅ Catalysts for Propane Oxidative Dehydrogenation (400 °C)

catalysts (V ₂ O ₅ wt %)	catalyst wt (mg)	conv of C ₃ H ₈ (%)	yield of C ₃ H ₆ (%)	sel to C ₃ H ₆	TOF of C ₃ H ₈ consumption (10 ⁻³ s ⁻¹)	rate (10 ⁻² μmol m ⁻² s ⁻¹)
Nb ₂ O ₅	100	0.04	0.04	100.0	0.1 ^a	0.02
1% V ₂ O ₅ /Nb ₂ O ₅	60	1.49	1.08	72.3	3.91	1.02
2% V ₂ O ₅ /Nb ₂ O ₅	60	3.57	2.55	71.3	4.67	2.46
3% V ₂ O ₅ /Nb ₂ O ₅	60	4.55	2.94	64.6	3.98	3.12
4% V ₂ O ₅ /Nb ₂ O ₅	30	3.34	2.01	60.0	4.38	4.86
5% V ₂ O ₅ /Nb ₂ O ₅	30	3.64	2.42	66.5	3.45	6.05
6% V ₂ O ₅ /Nb ₂ O ₅	30	3.54	2.57	72.9	3.10	6.08
8% V ₂ O ₅ /Nb ₂ O ₅	60	5.54	3.64	56.2	1.82 ^b	5.30
V ₂ O ₅	100	0.42	0.40	95.2	7.96 ^c	3.83

^a Density of active surface niobia sites of pure Nb₂O₅ was determined by 2-propanol chemisorption. ^b The V₂O₅ loading is greater than the monolayer. ^c Density of active surface vanadia sites of pure V₂O₅ was determined by 2-propanol chemisorption.^{37,38}

TABLE 4: Catalytic Properties of Supported MoO₃/Nb₂O₅ Catalysts for Propane Oxidative Dehydrogenation (450 °C)

catalysts (MoO ₃ wt %)	catalyst wt (mg)	conv of C ₃ H ₈ (%)	yield of C ₃ H ₆ (%)	sel to C ₃ H ₆	TOF of C ₃ H ₈ consumption (10 ⁻³ s ⁻¹)	rate (10 ⁻³ μmol m ⁻² s ⁻¹)
Nb ₂ O ₅	100	0.04	0.04	100.0	0.2 ^a	0.4
1% MoO ₃ /Nb ₂ O ₅	60	0.22	0.22	99.3	0.9	1.2
2% MoO ₃ /Nb ₂ O ₅	60	0.31	0.31	98.9	0.6	1.7
3% MoO ₃ /Nb ₂ O ₅	60	0.41	0.40	98.6	0.6	2.3
4% MoO ₃ /Nb ₂ O ₅	60	0.62	0.56	89.1	0.6	3.6
5% MoO ₃ /Nb ₂ O ₅	30	0.41	0.38	90.7	0.7	4.9
6% MoO ₃ /Nb ₂ O ₅	30	0.44	0.42	95.9	0.6	5.6
8% MoO ₃ /Nb ₂ O ₅	30	0.55	0.53	96.2	0.6	7.4
10% MoO ₃ /Nb ₂ O ₅	30	0.76	0.68	89.6	0.6	11.0
20% MoO ₃ /Nb ₂ O ₅	30	0.62	0.56	89.4	0.4 ^b	10.3
MoO ₃	100	0.03	0.03	98.2	1.8 ^c	2.0

^a Density of active surface niobia sites of pure Nb₂O₅ was determined by 2-propanol chemisorption. ^b The MoO₃ loading is greater than monolayer. ^c Density of active surface molybdena sites was determined by 2-propanol chemisorption.^{37,38}

reaction rate per unit surface area increases linearly with the vanadium oxide loading up to monolayer surface coverage (~5% V₂O₅/Nb₂O₅). Furthermore, the reaction rate normalized per surface vanadium oxide site, TOF, is essentially constant as a function of surface vanadia coverage below monolayer. According to previous structural characterization studies,⁴⁻⁶ the surface vanadia coverage has a significant effect on the structure of the surface vanadia species: isolated surface vanadia species are mainly present at low surface vanadia coverage whereas polymeric surface vanadia species are mainly present in the samples at high vanadia coverage (below monolayer). Therefore, the propane ODH reaction is a structure insensitive reaction that requires only one surface vanadia site for the activation of propane.

The catalytic properties of the model Nb₂O₅-supported molybdena catalysts for propane oxidation at 450 °C are presented in Figure 6. The selectivities to propylene for all the samples are very high (90–100%) for the chosen reaction conditions. The propane consumption rate linearly increases with molybdena loading until 10% MoO₃/Nb₂O₅. Thus, similarly to propane ODH over supported V₂O₅/Nb₂O₅ catalysts, the catalytic results suggest that ~10% MoO₃/Nb₂O₅ corresponds to monolayer coverage of surface molybdena species and that crystalline MoO₃ particles have a minimal effect on the reaction rate and propylene selectivity. The catalytic properties of supported MoO₃/Nb₂O₅ for propane ODH are summarized in Table 4. The TOF results further substantiate the conclusion that propane ODH is a structure insensitive reaction requiring only one surface MoO_x site.

3.4.2. Catalytic Activity of Bulk Mixed Metal Oxides. The influences of the V₂O₅, MoO₃, and TeO₂ contents on the propane ODH to propylene reaction over the bulk V–Nb–O, Mo–Nb–O, and Te–Nb–O mixed metal oxides were investigated at 400,

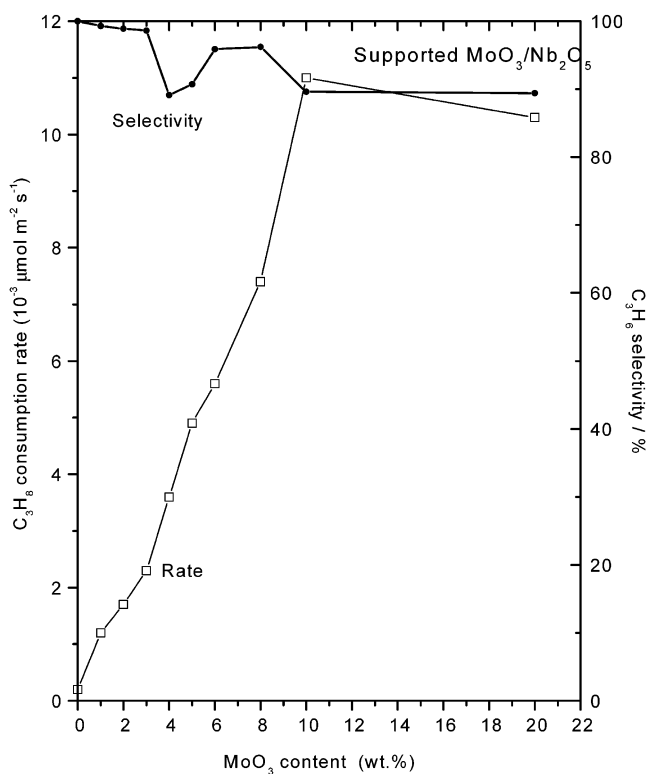


Figure 6. Oxidative dehydrogenation of propane over Nb₂O₅-supported molybdena metal oxides. Reaction at 450 °C; SF = 50 mL/min.

450, and 500 °C, respectively. Both propane conversion and propylene yield increased with increasing vanadia content in Nb₂O₅ and reached maxima at 10% V₂O₅. However, both catalytic parameters decreased upon further increasing the

TABLE 5: Catalytic Properties of Bulk V–Nb–O Mixed Metal Oxides for Propane Oxidative Dehydrogenation Reaction at 400 °C

catalysts	conv of C ₃ H ₈ (%)	sel to C ₃ H ₆ (%)	rate (10 ⁻² μmol m ⁻² s ⁻¹)	fraction of V on surface (%)	N _V (μmol m ⁻²)	TOF (10 ⁻³ s ⁻¹)
Nb ₂ O ₅	0.04	100	0.02		0.0	0.1 ^b
1% V–Nb–O	0.48	100	0.34	0.34	0.7	4.75
5% V–Nb–O	1.72	64.5	2.03	0.34	5.5	3.55
10% V–Nb–O	3.03	67.6	3.46	0.57	9.5	3.64
20% V–Nb–O	0.57	92.9	1.47	0.24	3.7	3.98
V ₂ O ₅	0.42	92.8	3.83		4.8 ^a	7.96

^a Number of active surface vanadia sites on pure V₂O₅ determined by 2-propanol chemisorption.^{37,38} ^b Calculated on the basis of the number of active surface niobia sites on pure Nb₂O₅ determined by 2-propanol chemisorption.^{37,38}

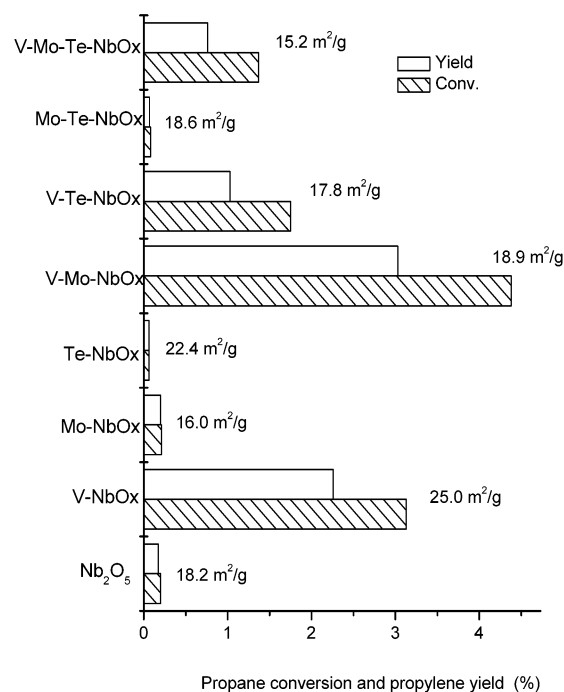
TABLE 6: Catalytic Properties of Bulk Mo–Nb–O Mixed Metal Oxides for Propane Oxidative Dehydrogenation Reaction at 450 °C

catalysts	conv of C ₃ H ₈ (%)	sel to C ₃ H ₆ (%)	rate (10 ⁻³ μmol m ⁻² s ⁻¹)	fraction of Mo on surface (%)	N _{Mo} (μmol m ⁻²)	TOF (10 ⁻³ s ⁻¹)
Nb ₂ O ₅	0.04	100	0.4		0.0	0.2 ^a
1% Mo–Nb–O	0.06	100	0.06	0.05	0.7	1.0
5% Mo–Nb–O	0.19	92.0	1.8	0.37	2.5	0.7
10% Mo–Nb–O	0.43	98.7	3.8	0.35	5.7	1.0
20% Mo–Nb–O	0.90	94.6	7.0	0.64	10.7	0.7
MoO ₃	0.03	98.2	2.0		3.6 ^b	0.6

^a Number of active surface niobis sites on pure Nb₂O₅ by 2-propanol chemisorption.^{37,38} ^b Number of active surface molybdena sites on pure MoO₃ by 2-propanol chemisorption.^{37,38}

vanadia content in the bulk V–Nb–O mixed metal oxides (see Table 5). In the Mo–Nb–O catalytic system, the catalytic activity does not change when 1% MoO₃ was introduced into the bulk Mo–Nb–O mixed metal oxide. However, both propane conversion and propylene yield rapidly increased with increasing molybdena content (see Table 6). The catalytic activities of all the samples in the Te–Nb–O system were extremely low and were even lower than pure Nb₂O₅. These results further confirm that telluria is completely inactive for propane activation to propylene. The catalytic properties of the bulk V–Nb–O and Mo–Nb–O mixed metal oxides for propane oxidative dehydrogenation are summarized in Tables 5 and 6, respectively. From the above results the activity order for propane ODH follows the trend V–Nb–O > Mo–Nb–O > Nb₂O₅ > Te–Nb–O.

The catalytic results for propane ODH reaction over the bulk V–Mo–Te–Nb–O mixed metal oxides at 500 °C are presented in Figure 7. Nb₂O₅ (TT) is a host matrix for these bulk mixed metal oxides because the contents for all the metal oxide components, except for Nb₂O₅, were limited to 1%. The propane conversion and propylene yield of pure Nb₂O₅ are very low. The propane conversion and propylene yield greatly increased when 1% V₂O₅ was introduced into the Nb₂O₅ (TT) matrix, suggesting that vanadia is an active component for propane activation. The catalytic behavior of 1% Mo–Nb–O was almost the same as that of pure Nb₂O₅. The catalytic activity significantly decreased when 1% TeO₂ was introduced into the Nb₂O₅ (TT) matrix. For the three-component samples, the catalytic activity of V–Mo–Nb–O was further enhanced compared to that of V–Nb–O, indicating that both V and Mo play important roles for propane oxidation and all the catalytic activities decreased when 1% TeO₂ was added to corresponding 2- or 3-multicomponent bulk mixed metal oxide catalyst (i.e., V–Mo–Te–Nb–O < V–Mo–Nb–O; Mo–Te–Nb–O < Mo–Nb–O; V–Te–Nb–O < V–Nb–O). These results suggest that telluria is an inactive component for propane ODH to propylene. The significant difference in catalytic activity of these bulk mixed metal oxides cannot be due to the differences in their surface areas because they are similar (see Figure 7).

**Figure 7.** Oxidative dehydrogenation of propane over bulk V–Mo–Te–Nb–O mixed metal oxides at 500 °C.

4. Discussion

4.1. Structural Models of Bulk and Supported Mixed Metal Oxides. The Raman and XRD characterization studies revealed that the synthesis of the bulk V–Nb–O, Mo–Nb–O, and Te–Nb–O mixed metal oxides followed three stages: (1) some cations were initially introduced into the bulk Nb₂O₅ (TT) lattice to form a solid solution or compound as well as present on the surface as surface metal oxide species, (2) a two-dimensional surface cation overlayer was formed after saturation of the solid solution, and (3) the formation of microcrystalline metal oxide phase (e.g., V₂O₅, MoO₃) after the completion of the surface metal oxide monolayer.

TABLE 7: Raman Band Positions of Dehydrated Surface M=O Terminal Bonds for Bulk V–Nb–O and Mo–Nb–O Mixed Metal Oxides and Their Corresponding Nb₂O₅-Supported Metal Oxides

sample	band position M=O (cm ⁻¹)	structure	substrate or support
Nb ₂ O ₅ (bulk)	not detected	polymeric NbO ₅ /NbO ₆	Nb ₂ O ₅ (TT)
1% V–Nb–O	not detected		Nb _{2-x} V _x O ₅ (TT)
5% V–Nb–O	980	polymeric VO ₆	Nb _{2-x} V _x O ₅ (TT)
10% V–Nb–O	1020 (~1025) ^a	polymeric VO ₄	V ₄ Nb ₁₈ O ₅₅ + Nb _{2-x} V _x O ₅
20% V–Nb–O	1020 (~1025) ^a	polymeric VO ₄	V ₄ Nb ₁₈ O ₅₅ + Nb _{2-x} V _x O ₅
surface NbO _x /Nb ₂ O ₅ ⁵⁶	~986	polymeric NbO ₅ /NbO ₆	Nb ₂ O ₅ (TT)
surface VO _x /V ₂ O ₅	~1020	Not known (polymeric VO ₄ ?)	V ₂ O ₅
1% V ₂ O ₅ /Nb ₂ O ₅ ^{5,54}	1031 ^a	isolated VO ₄	Nb ₂ O ₅
5% V ₂ O ₅ /Nb ₂ O ₅ ^{5,54}	1033 ^a	isolated VO ₄	Nb ₂ O ₅
1% Mo–Nb–O	not detected		Nb _{2-x} Mo _x O ₅ (TT)
5% Mo–Nb–O	~985 (very weak)	MoO ₆	Nb _{2-x} Mo _x O ₅ (TT)
10% Mo–Nb–O	987	MoO ₆	Nb _{2-x} Mo _x O ₅ (TT)
20% Mo–Nb–O	987	MoO ₆	Nb _{2-x} Mo _x O ₅ (TT)
5% MoO ₃ /Nb ₂ O ₅ ³⁶	996	MoO ₆	Nb ₂ O ₅ (TT)

^a Apparent Raman band position baseline corrected.

The Raman band positions and assignments for the terminal M=O bonds detected for the dehydrated surface metal oxide overlayers of the bulk V–Nb–O and Mo–Nb–O mixed metal oxides are summarized in Table 7. For comparison, the Raman bands for the corresponding dehydrated surface metal oxide species present in Nb₂O₅-supported oxides are also listed in Table 7. The very similar Raman band positions for the dehydrated surface metal oxide species on the bulk mixed metal oxides and their corresponding dehydrated Nb₂O₅-supported surface metal oxide species suggest that similar surface metal oxide species are also present on these bulk metal oxides. However, the surface metal oxide species on the bulk mixed metal oxides may not be exactly the same as those on the corresponding Nb₂O₅-supported metal oxides because the oxide supports or substrates are somewhat different in these two different types of systems. For example, as shown in Table 7, the substrate in the 5% V–Nb–O sample is the Nb_{2-x}V_xO₅ (TT) solid solution, and the substrate in 10% V–Nb–O is the V₄Nb₁₈O₅₅ compound, whereas for supported 5% V₂O₅/Nb₂O₅ the substrate is Nb₂O₅ (TT).

It is generally accepted that the bridging M–O–support bonds are kinetically critical for the catalytic activity of the supported metal oxides.^{4–6} However, the bridging V–O–support bond cannot be directly monitored with Raman or IR spectroscopy because it is not Raman active due to its slightly ionic character⁴⁸ and the IR absorption of the oxide supports also prevents its detection.⁴⁶ Fortunately, the different interactions between bridging bonds of V–O–support can be indirectly reflected by the terminal V=O Raman vibration. Thus, a good understanding of the terminal M=O bond can provide some structural information for determining the molecular structure model of the surface and bulk mixed metal oxides. For example, the Raman vibration of the terminal M=O is the most critical information for characterizing the surface species of supported metal oxides. For surface vanadia species, there are several factors that control the bond length of the terminal V=O bond and its Raman band position. The first factor is the number of terminal V=O bonds per vanadium atom. In this study, the possibility of dioxo (i.e., two terminal V=O bonds per vanadium atom) can be excluded because no Raman bands are detected around 920–950 cm⁻¹, which are characteristic of terminal dioxo V=O.^{49–51} The presence of terminal V=O Raman bands in the range 980–1030 cm⁻¹ indicate that only one terminal V=O bond per vanadium atom is present in the samples of this study. The second important factor affecting the terminal V=O vibration and its Raman band position is the number of oxygen atoms coordinated to vanadium. The lower the number

of oxygen ligands around the V cation, the higher the Raman band position, in cm⁻¹, of the terminal V=O bond. For instance, the vanadium cation has only 4-fold coordination in the isolated surface vanadyl species and exhibits the highest Raman band position (1030–1040 cm⁻¹).⁵⁷ The Raman band positions of terminal V=O bonds for polymeric surface vanadia species (coordination number of V cation ≥ 4-fold) are much lower than that of the isolated surface vanadia species and occur at ~1010–1020 cm⁻¹.⁵⁷ The V₂O₅ crystallites mostly consist of distorted VO₆/VO₅ units^{52,53} and exhibit a Raman band at 994 cm⁻¹ due to the terminal V=O bond. The third important factor is the character of the V–O–support bridging bond. The stronger the interaction of O–support in the bridging bond, the weaker the interaction of V–O in the bridging bond, therefore, the stronger the interaction of the terminal V=O bond, which results in a higher Raman band position (in cm⁻¹).

The Raman band of the terminal V=O bond of the surface vanadia species in the dehydrated 5% V–Nb–O sample was observed at 980 cm⁻¹, which is much lower than that of the surface vanadia species in the dehydrated 1% V₂O₅/Nb₂O₅ (~1031 cm⁻¹). Furthermore, the substrate for the surface vanadia species of 5% V–Nb–O is the V_xNb_{2-x}O₅ solid solution, in which the V atom has 6-fold coordination to adjacent oxygen atoms. These results suggest that the somewhat lower Raman band position may be due to the higher coordination number of vanadium cation in this surface vanadia species (probably 5 or 6). When the vanadia content increases to 10–20% V–Nb–O, a Raman band appears at ~1020 cm⁻¹ that is characteristic of (Nb–O)₃V=O structures. Furthermore, solid state ⁵¹V NMR studies of dehydrated V–Nb–O revealed that the surface VO_x species possesses VO₄ coordination and that the bulk VO_x species possesses VO₆ coordination.⁵⁴

Similar Raman band positions for dehydrated Mo–Nb–O and MoO₃/Nb₂O₅ suggest that similar molecular structures of the dehydrated surface MoO_x species are present in the bulk Mo–Nb–O mixed metal oxides and the supported MoO₃/Nb₂O₅ catalysts.^{36,55}

On the basis of the characterization results, the structural models of the surface species on the bulk mixed metal oxides are proposed and shown in Figure 8. For comparison, the structural model of corresponding Nb₂O₅-supported vanadia metal oxides, which have been extensively studied,^{4–6} are also shown in Figure 8.

4.2. Catalytic Model of the Bulk V–Nb–O and Mo–Nb–O Mixed Metal Oxides. As described in the Introduction, the bulk mixed metal oxides represent a very complex catalytic system. They possess three-dimensional structures, and Mⁿ⁺

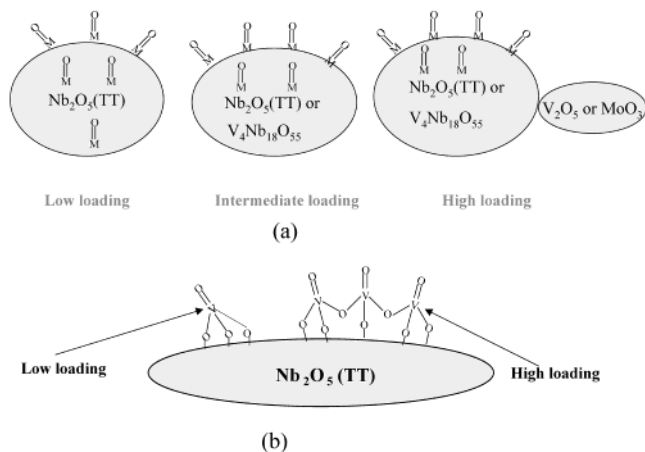


Figure 8. Structural models of surface species on bulk mixed oxides and on Nb₂O₅-supported vanadia metal oxides: (a) Bulk M–Nb–O (M = V, Mo); (b) V₂O₅/Nb₂O₅.

cations are present both in the bulk lattice and on the surface. In both bulk V–Nb–O and Mo–Nb–O mixed metal oxide catalysts, the highest propane conversions and propylene yields were found on the samples that possess the two-dimensional surface metal oxides. For example, the highest propane conversion and propylene selectivity were found on the 10% V–Nb–O and 20% Mo–Nb–O samples. These two samples exhibited the lowest XRD peak intensity of the bulk mixed metal oxides and the strongest Raman bands of the surface metal oxide species. These correlations strongly suggest that the surface metal oxide species are the active sites in these bulk mixed metal oxide catalysts.

The corresponding model Nb₂O₅-supported metal oxide catalysts were employed to determine the number of surface active sites present on the bulk V–Nb–O and Mo–Nb–O mixed metal oxides for propane oxidation on the basis of the following catalytic features and assumptions: (1) only the surface metal oxide species are the active sites for propane ODH because the bulk sites are not exposed to the reactants, (2) pure Nb₂O₅ has an extremely low activity for propane activation, indicating that only surface V or Mo oxide species are the active sites for V–Nb–O and Mo–Nb–O catalysts, respectively, (3) similar active surface sites are present in the bulk mixed metal oxides and their corresponding model Nb₂O₅-supported metal oxides.

The reaction rates normalized per unit surface area as a function of vanadia surface density for model Nb₂O₅-supported vanadia catalysts below monolayer coverage are presented in Figure 9. This standard curve can be used for the determination of the number of active surface V sites on bulk V–Nb–O mixed metal oxides by comparing the reaction rate per unit surface area under the same reaction conditions. The surface densities of the active surface vanadia species on the bulk V–Nb–O mixed metal oxides obtained by this method are listed in Table 5. Thus, the TOF values can be determined for the bulk mixed metal oxides after the numbers of surface vanadia sites on the bulk V–Nb–O mixed metal oxides are determined (see Table 5). The numbers of surface Mo atoms present on the bulk Mo–Nb–O mixed metal oxides were similarly determined by using the standard curve for the propane ODH reaction rate normalized per unit surface area as a function of molybdenum surface density of the corresponding model Nb₂O₅-supported molybdena catalysts (Figure 10). The results for the active surface molybdenum densities and TOF values of bulk Mo–Nb–O mixed metal oxides are presented in Table 6.

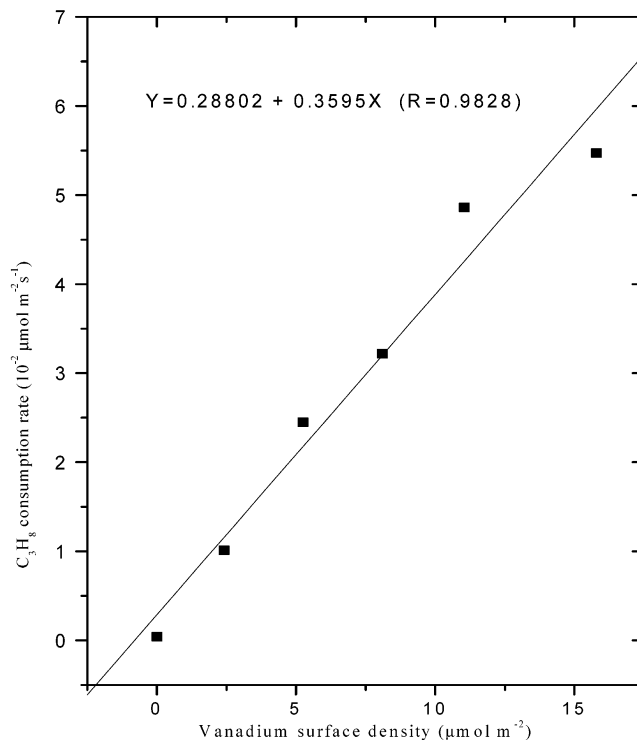


Figure 9. C₃H₈ consumption rate normalized per unit surface area as a function of vanadia surface density.

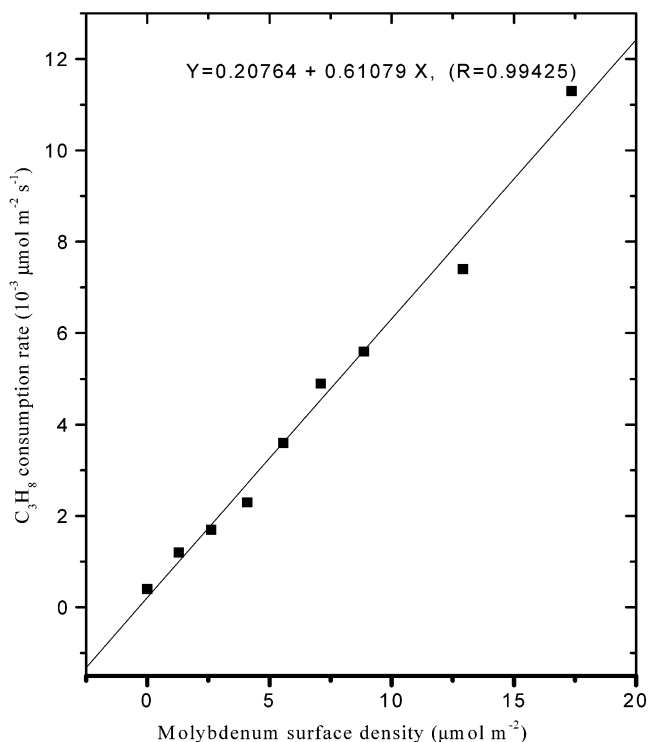


Figure 10. C₃H₈ consumption rate normalized per unit surface area as a function of molybdena surface density.

Comparison of the TOF values of the different metal oxide catalysts provides additional insight about the reactivity of the different active surface sites for propane ODH. The most active surface sites are found on bulk V₂O₅ crystals, only the surface vanadia sites at the edges are active,^{37,38} and are about twice as active as the surface vanadia sites present on the Nb₂O₅, V_xNb_{2-x}O₅, or V₄Nb₁₈O₅₅ bulk oxides. The surface vanadia sites are approximately 2 orders of magnitude more active than the

surface molybdena sites for propane ODH. The surface molybdena sites on bulk MoO₃ crystals (only the surface sites at the edges are active^{37,38}) are approximately 3 times as active as the surface molybdena sites present on the Nb₂O₅ or Mo_xNb_{2-x}O₅ bulk oxides. The surface molybdena sites are more than an order of magnitude more active than the surface niobia sites on bulk Nb₂O₅ for propane ODH. The surface telluria sites are even less active than the surface niobia sites. So the general specific activity trend of these surface metal oxide sites is VO_x ≫ MoO_x > NbO_x > TeO_x. This trend reveals that active catalysts for propane ODH must contain some surface vanadia sites.

The determination of the number of surface active sites of bulk mixed oxides by comparison with corresponding model supported metal oxides enabled the calculation of TOF and a reliable comparison of the catalytic behavior of different bulk mixed oxides. The composition and calcinations temperature of bulk mixed oxide catalysts affects the density of the surface active sites, which further controls their catalytic behavior.

5. Conclusions

(1) The bulk and surface structures of unsupported V–Nb–O and Mo–Nb–O mixed oxides were determined by XRD and Raman spectroscopy. The structural models of the surface species present on the bulk mixed metal oxides of V–Nb–O and Mo–Nb–O were proposed from comparative studies with the corresponding model Nb₂O₅-supported vanadia and molybdena.

(2) Propane ODH to propylene is a structure insensitive reaction because only one surface MO_x site is required for propane activation.

(3) The catalytic model for the bulk mixed metal oxides was proposed, and the surface vanadia and molybdena species are the active surface sites in the bulk V–Nb–O and Mo–Nb–O mixed metal oxide catalysts, respectively. The composition and calcination temperature of the bulk mixed oxide catalysts affects the surface density of the active sites, which controls their catalytic behavior.

(4) This is the first study to quantitatively determine the number of surface active sites present on bulk mixed metal oxides from a comparative study with the corresponding model supported metal oxides, which enabled the calculation of the TOF values and a reliable comparison of the catalytic behavior of different bulk mixed metal oxides.

(5) The reaction rate (μmol m⁻² s⁻¹) for the oxidative dehydrogenation of propane follows the pattern: V–NbO_x > Mo–NbO_x ≫ Nb₂O₅ > Te–NbO_x. Tellurium oxide is inactive for propane activation.

Acknowledgment. This work was supported by the U.S. Department of Energy, Basic Energy Sciences, Grant DE-FG02-93ER14350.

References and Notes

- (1) Ertl, G.; Knozinger, G.; Weitkamp, J., Eds. *Handbook of Heterogeneous Catalysis*; Wiley-VCH: Weinheim, 1997.
- (2) Kung, H. H. *Transition Metal Oxides, Surface Chemistry and Catalysis*; Elsevier: Amsterdam, 1989.
- (3) Brazdil, J. F. Bulk Metal Oxides. In *Characterization of Catalytic Materials*; Wachs, I. E., Ed.; Butterworth Heinemann: Boston, 1992; p 47.
- (4) Wachs, I. E.; Segawa, K. Supported Metal Oxides. In *Characterization of Catalytic Materials*; Wachs, I. E., Ed.; Butterworth Heinemann: Boston, 1992; p 69.
- (5) Wachs, I. E., Ed. Applications of Support Metal Oxide Catalysts. *Catal. Today* **1999**, *51*, 1.

- (6) Weckhuysen, B. M.; Wachs, I. E. Catalysis by Supported Metal Oxides. In *Handbook of Surface and Interfaces of Materials*; Nalwa H. S., Ed.; Academic Press: New York, 2001; Vol. 1, p 643.
- (7) Cavani, F.; and Trifiro, F. *Catal. Today* **1999**, *51*, 561.
- (8) Ertl, G.; Knozinger, G.; Weitkamp, J., Eds. *Environmental Catalysis*; Wiley-VCH: Weinheim, 1998.
- (9) Watling, T. C.; Deo, G.; Seshan, K.; Wachs, I. E.; Lercher, J. A. *Catal. Today* **1996**, *28*, 139.
- (10) Mamedov, E. A.; Corberan, V. C. *Appl. Catal. A: General* **1995**, *127*, 1.
- (11) Bettahar, M. M.; Costentin, G.; Savary, G.; Lavalley, J. C. *Appl. Catal. A: General* **1996**, *145*, 1.
- (12) Smits, R. H. H.; Seshan, K.; Ross, J. R.; Oetelaar, L. C. A.; Helweggen, J. H. J. M.; Anantharaman, Brongersma H. H. *J. Catal.* **1995**, *157*, 584.
- (13) Kung, M. C.; Kung, H. H. *J. Catal.* **1992**, *134*, 668.
- (14) Khodakov, A.; Yang, J.; Su, S.; Iglesia, E.; Bell, A. T. *J. Catal.* **1998**, *177*, 343.
- (15) Barbier, F.; Cauzzi, D.; Smet, F. D.; Devillers, M.; Moggi, P.; Predieri, G.; Ruiz, P. *Catal. Today* **2000**, *61*, 353.
- (16) Stern, D. L.; Grasselli, R. K. *J. Catal.* **1997**, *167*, 550.
- (17) Watson, R. B.; Ozkan, U. S. *J. Catal.* **2000**, *191*, 12.
- (18) Chen, K.; Xie, S.; Iglesia, E.; Bell, A. T. *J. Catal.* **2000**, *189*, 421.
- (19) Khodakov, A.; Olthof, B.; Bell, A. T.; Iglesia, E. *J. Catal.* **1999**, *181*, 205.
- (20) Chen, K.; Khodakov, A.; Yang, J.; Bell, A. T.; Iglesia, E., *J. Catal.* **2000**, *186*, 325.
- (21) Chen, K.; Xie, S.; Iglesia, E.; Bell, A. T. *J. Catal.* **2000**, *192*, 197.
- (22) Chen, K.; Bell, A. T.; Iglesia, E. *J. Phys. Chem. B* **2000**, *104*, 1292.
- (23) Lemonidou, A. A.; Nalbandian, L.; Vasalos, I. A. *Catal. Today* **2000**, *61*, 333.
- (24) Arena, F.; Frusteri, F.; Parmaliana, A. *Catal. Lett.* **1999**, *60*, 59.
- (25) Ermini, V.; Finocchio, E.; Sechi, S.; Busca, G.; Rossini, S. *Appl. Catal. A: General* **2000**, *198*, 67.
- (26) Lopez Nieto, J. M.; Coenraads, R.; Dejoz, A.; Vazquez, M. I. *Stud. Surf. Sci. Catal.* **1997**, *110*, 443.
- (27) Gao, X.; Jehng, J. M.; Wachs, I. E. *J. Catal.* **2002**, *209*, 43.
- (28) Eon, J. G.; Olier R.; Volta, J. C. *J. Catal.* **1994**, *145*, 318.
- (29) Banares, M. A. *Catal. Today* **1999**, *51*, 319.
- (30) Banares, M. A.; Gao, X.; Fierro, J. L. G.; Wachs, I. E. *Stud. Surf. Sci. Catal.* **1997**, *110*, 295.
- (31) Blasco, T.; Galli, A.; Lopez Nieto, J. M.; Trifiro, F. *J. Catal.* **1997**, *169*, 203.
- (32) Oyama, S. T.; Somorjai, G. A. *J. Phys. Chem.* **1990**, *94*, 5022.
- (33) Oyama, S. T. *J. Catal.* **1991**, *128*, 210.
- (34) Ushikuba, T.; Oshima, K.; Kayou, A.; Vaarkamp, M.; Hatano, M. *J. Catal.* **1997**, *169*, 394.
- (35) Gao, X.; Bare, S.; Weckhuysen, B. M.; Wachs, I. E. *J. Phys. Chem. B* **1998**, *102*, 10842.
- (36) Hu, H.; Wachs, I. E. *J. Phys. Chem.* **1995**, *99*, 10897.
- (37) Kulkarni, D.; Wachs, I. E. *Appl. Catal. A: General* **2002**, *237*, 121.
- (38) Badlani, M.; Wachs, I. E. *Catal. Lett.* **2001**, *75*, 137.
- (39) XRD standard data in JCPDS, No. 28-0317.
- (40) XRD standard data in JCPDS, No. 46-0087.
- (41) Jehng, J. M.; Wachs, I. E. *Catal. Today* **1990**, *8*, 37.
- (42) Ikeya, T.; Senna, M. *J. Non-Cryst. Solids* **1998**, *105*, 243.
- (43) Wachs, I. E.; Briand, L. E.; Jehng, J. M.; Burcham, L.; Gao, X. *Catal. Today* **2000**, *57*, 323.
- (44) Wachs, I. E.; Jehng, J. M.; Deo, G.; Hu, H.; Arora, N. *Catal. Today* **1996**, *28*, 199.
- (45) Weast, R. C.; Astle, M. J.; Beyer, W. H., Eds. *Handbook of Chemistry and Physics*; CRC Press: 1986; p F-157.
- (46) Machej, T.; Haber, J.; Turek, A. M.; Wachs, I. E. *Appl. Catal.* **1991**, *90*, 194.
- (47) Wang, C.-B.; Cai, Y.; Wachs, I. E. *Langmuir* **1999**, *20*, 111.
- (48) Wachs, I. E. *Catal. Today* **1996**, *27*, 437.
- (49) Cristiani, C.; Forzatti, P.; Busca, G. *J. Catal.* **1989**, *116*, 586.
- (50) Beattie, I. R.; Wickins, T. D. *J. Chem. Soc. A* **1969**, 1087.
- (51) Zhao, Z.; Yamada, Y.; Teng, Y.; Ueda, A.; Nakagawa, K.; Kobayashi, T. *J. Catal.* **2000**, *190*, 215.
- (52) Wells, A. F. *Structural Inorganic Chemistry*, 5th ed.; Clarendon Press: Oxford, U.K., 1984; p 568.
- (53) Haber, J.; Witko, M.; Tokarz, R. *Appl. Catal. A: General* **1997**, *157*, 3.
- (54) Jehng, J.-M.; Wachs, I. E.; Eckert, H. Unpublished results.
- (55) Hu, H.; Wachs, I. E. *J. Phys. Chem.* **1995**, *99*, 10911.
- (56) Jehng, J.-M.; Wachs, I. E. *Chem. Mater.* **1991**, *3*, 100.
- (57) Burcham, L. J.; Gao, X.; Deo, G.; Wachs, I. E. *Top. Catal.* **2000**, *11/12*, 85.